

ROBUST CONTROL OF AN ISOLATED HYBRID WIND-DIESEL POWER SYSTEM USING LINEAR QUADRATIC GAUSSIAN APPROACH

Ahmed. M. Kassem

Control Technology Dep., Bini-Swief University, Egypt,

Email: Kassem_ahmed53@hotmail.com

(Received December 13, 2008 Accepted March 12, 2009)

This paper presents the application of the Linear Quadratic Gaussian (LQG) controller for voltage and frequency regulation of an isolated hybrid wind-diesel scheme. The scheme essentially consists of a vertical axis wind turbine driving a self-excited induction generator connected via an asynchronous (AC-DC-AC) link to a synchronous generator driven by a diesel engine. The synchronous generator is equipped with a voltage regulator and a static exciter. The wind generator and the synchronous generator together cater for the local load and power requirement. However, the load bus voltage and frequency are governed by the synchronous generator. The control objective aims to regulate the load voltage and frequency. This is accomplished via controlling the field voltage and rotational speed of the synchronous generator. The complete nonlinear dynamic model of the system has been described and linearized around an operating point. The standard Kalman filter technique has been employed to estimate the full states of the system. The computational burden has been minimized to a great extent by computing the optimal state feedback gains and the Kalman state space model off-line. The proposed controller has the advantages of robustness, fast response and good performance. The hybrid wind diesel energy scheme with the proposed controller has been tested through a step change in both wind speed and load impedance. Simulation results show that accurate tracking performance of the proposed hybrid wind diesel energy system has been achieved.

KEYWORDS: wind turbine, induction generator, synchronous generator, robust control and LQG control.

NOMENCLATURE

v_{ds}, v_{qs}	d-q stator voltages of induction generator,
i_{ds}, i_{qs}	d-q stator currents of induction generator,
i_{dr}, i_{qr}	d-q rotor currents of induction generator,
R_s, R_r	stator and rotor resistances per phase of induction generator,
L_s, L_r, L_m	stator, rotor and magnetizing inductances of induction generator

C_0	self excitation capacitance per phase of induction generator
ω_s	Angular stator frequency of the induction generator
ω_m	Angular rotor speed (electrical rads/s) of the induction generator
J	moment of inertia,
f	friction coefficient,
p	differential operator d/dt
L_{DC}	DC-link inductance
R_{DC}	DC-link resistance
α_R, α_I	firing angles of the converter and inverter.
v_{dcon}, v_{qcon}	d-q input voltage of the converter.
i_{dcon}, i_{qcon}	d-q input current of the converter.
I_{DC}	DC-link current.
v_{inv}	inverter output voltage
v_d^r, v_q^r	d-q stator voltages of synchronous generator,
v_{kd}^r, v_{kq}^r	d-q damper winding voltages of synchronous generator,
v_f^r	field winding voltage of synchronous generator,
i_d^r, i_q^r	d-q stator currents of synchronous generator,
i_{kd}^r, i_{kq}^r	d-q damper winding currents of synchronous generator,
i_f^r	field winding current of synchronous generator,
R_s	stator resistance of synchronous generator,
R_{kd}, R_{kq}	d and q damper winding resistances,
L_{md}, L_{mq}	d and q mutual inductances,
L_d, L_q	d and q self inductances,
ω_{sg}	rotor speed (electrical rads/s) of the synchronous generator,
T_{md}	torque input from diesel engine,
φ_r, φ_f	applied and actual fuel flow rate of diesel engine,
τ_1	combustion delay time constant,
τ_2, K_2	time constant and gain of fuel rack position actuator,

1. INTRODUCTION

During last three decades, the assessment of potential of the sustainable eco-friendly alternative sources and refinement in technology has taken place to a stage so that economical and reliable power can be produced. Different renewable sources are available at different geographical locations close to loads, therefore, the latest trend is to have distributed or dispersed power system. Example of such systems is wind-diesel. This system is known as hybrid power systems.

The advantage of hybrid power systems is the combination of the continuously available diesel power and locally available, pollution-free wind energy. With the hybrid power system, the annual diesel fuel consumption can be reduced and, at the same time, the level of pollution can be minimized. A proper control strategy has to be developed to take full advantage of the wind energy during the periods of time it is available and to minimize diesel fuel consumption. Therefore, a proper control system has to be designed, subject to the specific constraints for a particular application. It has to maintain power quality, measured by the quality of electrical performance, i.e., both the voltage and the frequency have to be properly controlled [1]. These results in a need for a simulation study of each new system to confirm that a control strategy results in desired system performance.

The wind-diesel systems are normally equipped with a control system, which functions to reduce the system frequency oscillations, when the system is subjected to wind/load disturbances [2].

Various control strategies have concerned with the voltage and/or frequency control of the hybrid wind-diesel power system and achieving optimal out of the turbine. In some schemes, the hybrid wind-diesel power system uses compressed air energy storage with the wind-diesel hybrid system [3]. Other control schemes use static VAR compensators for reactive power control [4]. Mathematical modeling of a typical hybrid system with PI controllers and system dynamic studies on it has been reported by Scott [5]. However, it is well known that the performance of the systems with fixed gain controllers designed on the fixed parameter model of the system does not stay optimal as the system parameters undergo a change.

Recently, advanced control techniques, which were applied successfully on the machine drives, have been proposed for regulating the wind power in a grid connected wind energy conversion scheme. They include Artificial neural networks [6-8], fuzzy control [7-9] and vector control [10]. In these methods, the speed feedback may be necessary to avoid instability. Moreover, wind velocity information may be needed as well. Also, the key point of direct power schemes is a correct and fast estimation of the active and reactive power as well as fast PI controllers.

In this paper, a controller design and simulations of a wind-diesel generation plant based on LQG approach are presented. This generation plant is conceived to supply electric power to an isolated load not connected to the electrical network. The main power generation system consists of a wind turbine driving a self-excited induction generator connected via an asynchronous DC link to a synchronous generator driven by a diesel engine. The synchronous generator is equipped with a voltage regulator and a static exciter. The wind generator and the synchronous generator together feed the local load.

The proposed hybrid wind diesel energy scheme with the proposed controller has been tested through a step change in both wind speed and load impedance. Simulation results show that there is accurate tracking performance of the proposed hybrid wind diesel energy system.

2. SYSTEM DESCRIPTION

Figure 1 shows a hybrid wind-diesel interface scheme, to supply a local isolated load. The scheme essentially consists of a vertical axis wind turbine driving a self-excited

induction generator (SEIG) connected via an asynchronous (AC-DC-AC) link to a synchronous generator driven by a diesel engine. The synchronous generator is equipped with a voltage regulator and a static exciter. The wind generator and the synchronous generator together feed the local load power requirement.

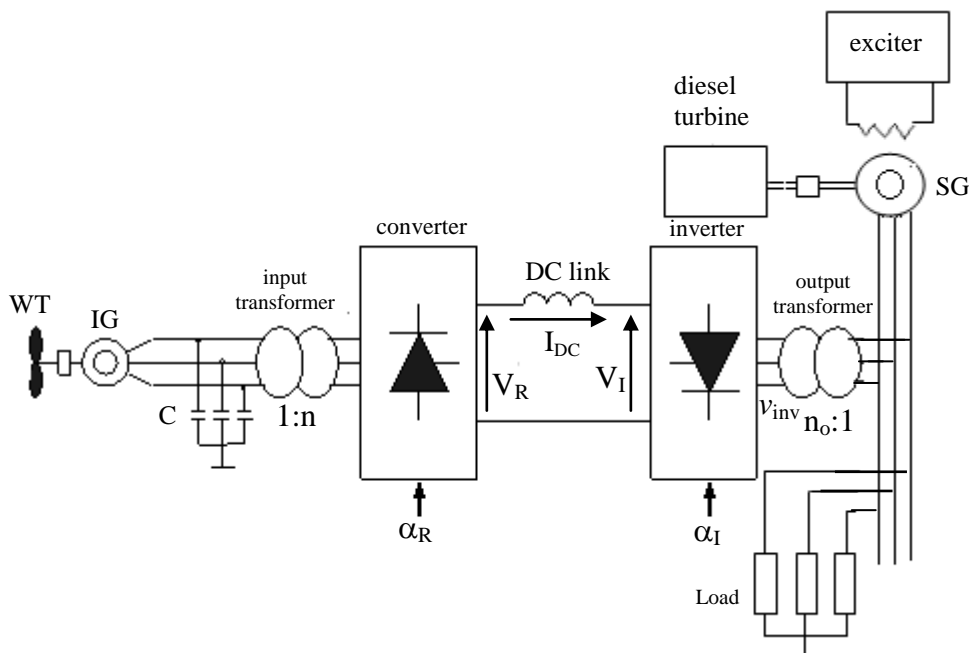


Fig. 1: Block Schematic diagram of the proposed hybrid wind-diesel-generation system.

3. SYSTEM DYNAMIC MODEL

The dynamic models of the different parts of the system can be described as follows:

3.1 Wind Side Dynamic Model

The wind side system consists of wind turbine, induction generator and DC-Link which can model as following:

3.2 Wind turbine Dynamic Model

The wind turbine is characterized by no dimensional curves of the power coefficient C_p as a function of both the tip speed ratio, λ and the blade pitch angle, β . In order to fully utilize the available wind energy, the value of λ should be maintained at its optimum value. Hence, the power coefficient corresponding to that value will become maximum also.

The tip speed ratio λ can be defined as the ratio of the angular rotor speed of the wind turbine to the linear wind speed at the tip of the blades. It can be expressed as follows:

$$\lambda = \omega_t R / V_w \tag{1}$$

Where R is the wind turbine rotor radius, v_w is the wind speed and ω_t is the mechanical angular rotor speed of the wind turbine.

The torque available from the wind turbine can be expressed as [11] :

$$T_m = 0.5\rho A R \left[\left(0.44 - 0.0167\beta \right) \sin \left(\frac{\frac{\omega_t R}{V_w} - 3}{15 - 0.3\beta} \right) - 0.00184 \left(\frac{\omega_t R}{V_w} - 3 \right) \beta \right] V_w^3 / \omega_t \tag{2}$$

Where ρ is the air density, and A is the swept area by the blades.

3.1.2 Induction Generator Dynamic Model

The dynamic behavior of the induction generator in the d-q axis synchronously rotating reference frame is given by [12] :

$$p i_{qs} = -R_s A_1 i_{qs} - (\omega_s + A_2 \omega_m L_m) i_{ds} + R_r A_2 i_{qr} - A_1 \omega_m L_r i_{dr} \tag{3}$$

$$p i_{ds} = (\omega_s + A_2 \omega_m L_m) i_{qs} - R_s A_1 i_{ds} + R_r A_2 i_{dr} + A_1 \omega_m L_m i_{qr} - A_1 v_{ds} \tag{4}$$

$$p i_{qr} = R_s A_2 i_{qs} + A_2 \omega_m L_s i_{ds} - A_3 i_{qr} + (-\omega_s + A_1 \omega_m L_s) i_{dr} \tag{5}$$

$$p i_{dr} = -A_2 \omega_m L_s i_{qs} + R_s A_2 i_{ds} + (\omega_s - A_1 \omega_m L_s) i_{qr} - A_3 i_{dr} + A_2 v_{ds} \tag{6}$$

Where $v_{qs} = 0$, due to the choice of axis alignment, and

$$A_1 = L_r / (L_s L_r - L_m^2), \quad A_2 = L_m / (L_s L_r - L_m^2),$$

and $A_3 = R_r (1 + A_2 L_m) / L_r$

The rotor speed ω_m is governed by the following differential equation:

$$T_m + T_e = (Jp + f) \omega_m / P \tag{7}$$

Where P is number of poles of the induction generator, T_m is the input torque from the prim-mover, and T_e is the electromagnetic torque representing the load on the induction generator (T_e is negative for generator action) which is given by :

$$T_e = 1.5 P L_m (i_{qs} i_{dr} - i_{ds} i_{qr}) \tag{8}$$

Equations (9) and (10) are combined as

$$p \omega_m = (-f \omega_m + P T_m + 1.5 P^2 L_m (i_{qs} i_{dr} - i_{ds} i_{qr})) / J \tag{9}$$

3.1.3 Asynchronous DC Link Model

The asynchronous DC link (used to interface the wind energy system to the utility) consists of a six pulse line commutated converter, a smoothing reactor, and a six pulse line commutated inverter. An isolating transformer of turns ratio $1 : n$ interconnects the induction generator to the converter. Neglecting the resistance and leakage reactance of the isolating transformer, the various ac quantities on the primary and secondary sides can be related by:

$$v_{dcon} = n v_{ds}, \quad v_{qcon} = n v_{qs}, \quad i_{qcon} = i_{qt} / n, \quad i_{dcon} = i_{dt} / n \tag{10}$$

Assuming the converter is lossless, the instantaneous power balance equation ($v_{qcon} = 0$, due to the choice of axis alignment) :

$$\frac{3}{2} v_{dcon} i_{dcon} = V_R I_{DC} \tag{11}$$

Where V_R is the DC voltage at the converter output terminals which can be written as :

$$V_R = \frac{3\sqrt{3}}{\pi} n v_{ds} \cos \alpha_R \tag{12}$$

The ac and dc currents of the converter are related by :

$$i_{con} = \sqrt{(i_{qcon}^2 + i_{dcon}^2)} = \frac{2\sqrt{3}}{\pi} I_{DC} \tag{13}$$

Neglecting the commutation overlap, the d-q converter currents can be deduced using equations (13-15) as :

$$i_{dcon} = i_{con} \cos \alpha_R = \frac{2\sqrt{3}}{\pi} I_{DC} \cos \alpha_R \tag{14}$$

$$i_{qcon} = -i_{con} \sin \alpha_R = -\frac{2\sqrt{3}}{\pi} I_{DC} \sin \alpha_R \tag{15}$$

Referring to Fig. 1, the dynamics introduced by the DC link is given by:

$$L_{DC} p I_{DC} + R_{DC} I_{DC} = V_R - V_I \tag{16}$$

Where v_I is the DC voltage at the inverter input terminals which can be expressed as:

$$V_I = -\frac{3\sqrt{3}}{\pi} v_{inv} \cos \alpha_I + \frac{3x_{ci}}{\pi} I_{DC} \tag{17}$$

where x_{ci} is the commutating reactance.

Combining equations (12), (17), and (18) the following equation can be obtained :

$$p I_{DC} = (-R_{DC} I_{DC} + \frac{3\sqrt{3}}{\pi} n v_{ds} \cos \alpha_R + \frac{3\sqrt{3}}{\pi} v_{inv} \cos \alpha_I - \frac{3x_{ci}}{\pi} I_{DC}) / L_{DC}$$

$$p I_{DC} = \left(\begin{array}{l} \left(-R_{DC} - \frac{3x_{ci}}{\pi} - \frac{18R_L}{\pi^2} (\cos(\alpha_I))^2 - \frac{18\omega_e L_L}{\pi^2} (\sin(\alpha_I))^2 \right) I_{DC} \\ + \frac{3\sqrt{3}}{\pi} n \cos \alpha_R v_{ds} + \frac{3\sqrt{3}n_o}{\pi} \cos \alpha_I \begin{pmatrix} i'_q \cos(\delta) + i'_d \sin(\delta) \\ -i'_q \sin(\delta) + i'_d \cos(\delta) \end{pmatrix} \end{array} \right) / L_{DC} \tag{18}$$

3.1.4 Self Excitation Capacitor Model

Referring to the d-q equivalent circuit of the self excitation capacitor shown in Fig. 2, the following differential equations can be written:

$$p v_{qs} = \frac{i_{qc}}{C_0} - \omega_s v_{ds} \tag{19}$$

$$p v_{ds} = \frac{i_{dc}}{C_0} + \omega_s v_{qs} \tag{20}$$

Since, $v_{qs} = 0$, due to the choice of axis alignment, equations (21-22) can be rewritten as:

$$\omega_s = \frac{i_{qc}}{C_0 v_{ds}} \tag{21}$$

$$p v_{ds} = \frac{i_{dc}}{C_0} \tag{22}$$

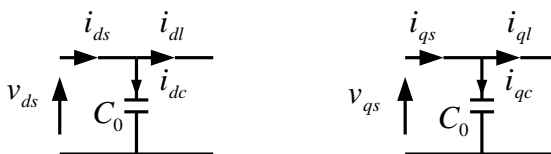


Fig. 2 : d-q equivalent circuit of the self excitation capacitor

Referring to Fig. 2, the values of i_{qc} and i_{dc} can be written as:

$$i_{qc} = i_{qs} - i_{ql} \quad , \quad i_{dc} = i_{ds} - i_{dl} \tag{23}$$

Equations (12, 15 and 16) are combined with equation (25) as:

$$i_{qc} = i_{qs} + \frac{2\sqrt{3}}{\pi} nI_{DC} \sin\alpha_R \quad , \quad i_{dc} = i_{ds} - \frac{2\sqrt{3}}{\pi} nI_{DC} \cos\alpha_R \tag{24}$$

Substituting the values of i_{qc} and i_{dc} from equation (26) into equations (23) and (24) would give:

$$\omega_s = \frac{i_{qs} + \frac{2\sqrt{3}}{\pi} nI_{DC} \sin\alpha_R}{C_0 v_{ds}} \tag{25}$$

$$p v_{ds} = \frac{i_{ds} - \frac{2\sqrt{3}}{\pi} nI_{DC} \cos\alpha_R}{C_0} \tag{26}$$

Equation (27) can be used to determine the electrical frequency of the voltage generated by the induction generator.

3.3 Diesel Side Dynamic Model

Diesel side system consists of diesel engine, synchronous generator and the load which can modeled as following:

3.2.1 Synchronous Generator Dynamic Modeling

The dynamic behavior of the synchronous generator in the d^f - q^f axis synchronously rotating reference frame fixed in the rotor (i.e., d^f - q^f reference frame rotating at the rotor speed ω_{sg}) is given by [12]:

$$p i_q^r = \left(\frac{L_{kq}}{L_{kq} - L_{mq}^2} \right) \left[-R_s i_q^r - \frac{L_{kq} L'_{mq}}{L_{kq}} i_{kq}^{r'} - \omega_{sg} i_d^r + \omega_{sg} L_{md} i_{kd}^{r'} + \omega_{sg} L_{md} i_f^{r'} - v_q^r \right] \dots \tag{27}$$

$$p i_d^r = \frac{1}{K_{11}} \left[\begin{aligned} &\omega_{sg} L_q i_q^r - R_s i_d^r - \omega_{sg} L_{mq} i_{kq}^{r'} \\ &+ (K_{22} R'_{kd} L'_f + K_{33} R'_{kd} L_{md}) i_{kd}^{r'} \\ &- (K_{22} L_{md} + K_{33} L'_{kd}) R'_f i_f^{r'} \\ &+ (K_{22} L_{md} + K_{33} L'_{kd}) v_f^r - v_d^r \end{aligned} \right] \tag{28}$$

$$p i_{kq}^{r'} = -\frac{R'_{kq}}{L'_{kq}} i_{kq}^{r'} + K_{44} \left[\begin{aligned} &-R_s i_q^r - \frac{R'_{kq} L_{mq}}{L'_{kq}} i_{kq}^{r'} - \omega_{sg} L_d i_d^r \\ &+ \omega_{sg} L_{md} i_{kd}^{r'} + \omega_{sg} L_{md} i_f^{r'} - v_q^r \end{aligned} \right] \tag{29}$$

$$p i_{kd}^{r'} = K_{22} \left[v_f^{r'} + \frac{(L_{md} - L_f')}{K_{11}} \begin{pmatrix} \omega_{sg} L_q i_q^r - R_s i_d^r - \omega_{sg} L_{mq} i_{kq}^{r'} \\ + (K_{22} L_f' R_{kd}' + K_{33} L_{md} R_{kd}') i_{kd}^{r'} \\ - (K_{22} L_{md} R_{kd}' + K_{33} L_f') R_f' i_f^{r'} \\ + (K_{22} L_{md} R_{kd}' + K_{33} L_{kd}') v_f^{r'} - v_d^r \\ + \frac{R_{kd}' L_f'}{L_{md}} i_{kd}^{r'} - R_f' i_f^{r'} \end{pmatrix} \right] \dots \dots \dots (30)$$

$$p i_f^{r'} = \frac{L_{kd}'}{L_{md}} K_{33} \left[v_f^{r'} + \frac{1}{K_{11} K_{55}} \begin{pmatrix} \omega_{sg} L_q i_q^r - R_s i_d^r - \omega_{sg} L_{mq} i_{kq}^{r'} \\ + (K_{22} L_f' R_{kd}' + K_{33} L_{md} R_{kd}') i_{kd}^{r'} \\ - (K_{22} L_{md} + K_{33} L_{kd}') R_f' i_f^{r'} \\ + (K_{22} L_f' R_{kd}' + K_{33} L_{md} R_{kd}') v_f^{r'} - v_d^r \\ + \frac{R_{kd}' L_{md}}{L_{kd}'} i_{kd}^{r'} - R_f' i_f^{r'} \end{pmatrix} \right] \dots \dots \dots (31)$$

Where

$$K_{11} = L_d - \frac{L_{md}^2 (L_{md} - L_f')}{(L_{md}^2 - L_f' L_{kd}')} - \frac{L_{md} (L_{md} L_{kd}' - L_{md}^2)}{(L_f' L_{kd}' - L_{md}^2)}$$

$$K_{22} = \left(\frac{L_{md}}{L_{md}^2 - L_f' L_{kd}'} \right), \quad K_{33} = \left(\frac{L_{md}}{L_f' L_{kd}' - L_{md}^2} \right), \quad K_{44} = \left(\frac{L_{mq}}{L_q L_{kq} - L_{mq}^2} \right), \quad K_{55} = \left(\frac{L_{kd}'}{L_{md} L_{kd}' - L_{md}^2} \right),$$

The q^r and d^r stator voltages in the reference frame fixed in the rotor are given by:

$$v_q^r = -i_q^r R_s - \omega_{sg} L_d i_d^r + \omega_{sg} L_{md} i_{kd}^{r'} + \omega_{sg} L_{md} i_f^{r'} \quad (32)$$

$$v_d^r = -i_d^r R_s + \omega_{sg} L_q i_q^r - \omega_{sg} L_{mq} i_{kq}^{r'} \quad (33)$$

The rotor speed ω_{sg} is governed by the following differential equation:

$$\frac{2}{P_o} (J p \omega_{sg} + f \omega_{sg}) = T_{md} - T_e \quad (34)$$

Where, P_o is the number of poles of synchronous generator, T_{md} is the input torque from the prime mover (diesel engine) and T_e is the electromagnetic torque representing the electrical load on the synchronous generator and is given by :

$$T_e = \left(\frac{3}{2} \right) \left(\frac{P_o}{2} \right) \left[L_{md} (-i_d^r + i_f' + i_{kd}') i_q^r - L_{mq} (-i_q^r + i_{kq}') i_d^r \right] \quad (35)$$

Lastly, the torque angle representing the electrical load on the synchronous generator is given by:

$$p \delta = \frac{2}{P_o} (\omega_{sg} - \omega_e) + \delta_o \quad (36)$$

Where ω_{sg} and ω_e are the synchronous generator's rotor speed and electrical frequency respectively and δ_o is the initial torque angle. In steady state, ω_{sg} and ω_e are the same, but during transient ω_{sg} changes and ultimately settles down to the value ω_e . The v_q^e and v_d^e stator voltages in the reference frame fixed with the synchronously rotating frame MMF vector rotating at an angular velocity ω_e are given by:

$$v_q^e = v_q^r \cos(\delta) + v_d^r \sin(\delta) \quad (37)$$

$$v_d^e = -v_q^r \sin(\delta) + v_d^r \cos(\delta) = 0 \quad (38)$$

$$v_L = \sqrt{(v_q^e)^2 + (v_d^e)^2} = v_q^e \quad (39)$$

The initial orientation of q and d reference frame is chosen such that v_d^e is initially zero and the load voltage $V_L = v_q^e$.

3.2.2 Voltage Regulator and Static Exciter Model

The voltage and frequency at the local load bus are set by the synchronous generator. Under load excursion, the load voltage tends to vary. In order to regulate the bus voltage, the synchronous generator is equipped with an automatic voltage regulator (AVR) and a static exciter [12]. The static exciter is an "inverted" three phase generator, with the automatic windings on the rotor and the field windings on the stator. The AC armature voltage is rectified using diodes mounted on the rotating shaft, and the rectified voltage is applied to the synchronous generator field as shown in fig. 3. The differential equations describing the excitation system for the synchronous generator are as follows:

$$pv_c = (V_{Lref} - V_L) = V_{ref} - \left\{ \begin{aligned} &R_L \left(i_q^r \cos(\delta) + i_d^r \sin(\delta) - \frac{2\sqrt{3}}{\pi n_o} I_{DC} \cos(\alpha_i) \right) \\ &+ \omega_e L_L \left(-i_q^r \sin(\delta) + i_d^r \cos(\delta) - \frac{2\sqrt{3}}{\pi n_o} I_{DC} \sin(\alpha_i) \right) \end{aligned} \right\} \tag{40}$$

$$pv'_{f'} = \frac{K_e v_c - v'_{f'}}{\tau_e} \tag{41}$$

Where, K_e is the gain of the exciter and τ_e is the time constant of the exciter.

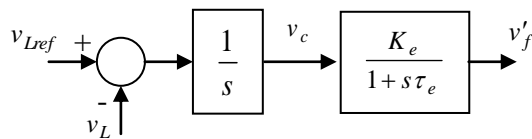


Fig. 3: Static voltage regulator loop

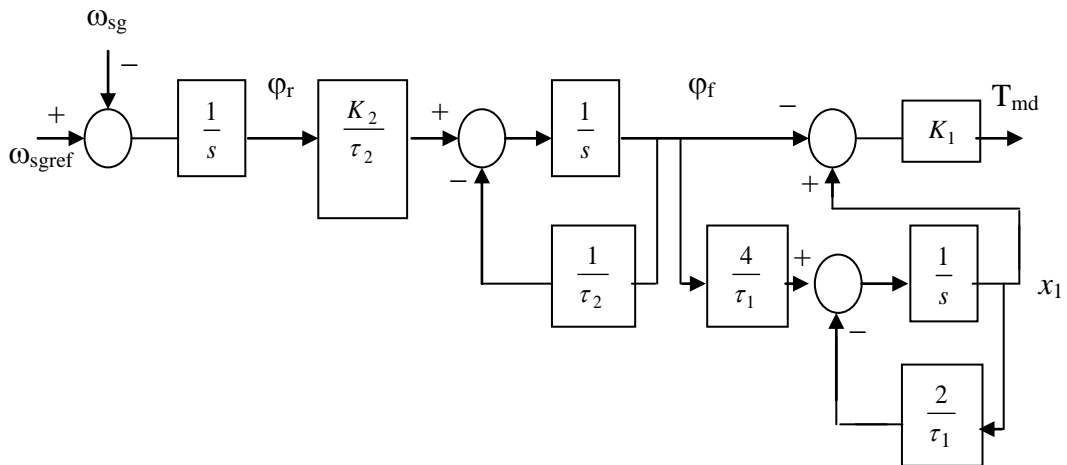


Fig.4: State space representation of diesel engine and speed regulator loop

3.2.3 Speed Regulator And Diesel Engine Model

The synchronous generator is driven by a diesel engine which controls the mechanical power input to the generator to balance the electrical load on the machine. If the electrical load on the generator changes due to change in power drawn by the local load, the rotor speed and hence the electrical frequency tend to change. In such a situation the mechanical power (or torque) input to the synchronous generator is controlled to regulate the system electrical frequency. The block diagram of the diesel engine is shown in fig. 4 [12]. The input signal is the speed (frequency) error and is used to determine the applied fuel flow rate ϕ_r depending on the position of the fuel rack which is controlled by the fuel actuator, characterized by a gain k_2 and a time constant τ_2 . The torque output T_{md} of the diesel engine is proportional to the actual fuel flow rate ϕ_f , but is delayed by the fuel combustion process time delay τ_1 . The torque output of the diesel engine is:

$$T_{md} = K_1 \phi_f e^{-\tau_1 s} \quad (42)$$

Where K_1 is constant relating the torque output to the fuel flow rate. The combustion process delay can be approximated using first order Pad's approximation as follows:

$$e^{-\tau_1 s} = \frac{\left(\frac{2}{\tau_1} - s \right)}{\left(\frac{2}{\tau_1} + s \right)} \quad (43)$$

The actual fuel flow rate ϕ_f is dependent on the applied fuel flow rate ϕ_r and is given by:

$$\phi_f = \frac{K_2}{(1 + \tau_2 s)} \phi_r \quad (44)$$

Where K_2 and τ_2 are gain and time constant of the fuel actuator. The differential equations describing the diesel engine and its speed governor are given by [12]:

$$p\phi_r = \omega_{sgref} - \omega_{sg} \quad (45)$$

$$p\phi_f = \frac{K_2 \phi_r - \phi_f}{\tau_2} \quad (46)$$

$$p x_1 = \frac{4\phi_f - 2x_1}{\tau_1} \quad (47)$$

$$T_{md} = K_1(x_1 - \phi_f) \quad (48)$$

3.3 Small Signal Linearized model

The subsystem models can be interfaced to form the unified nonlinear model.

The nonlinear model of the hybrid wind-diesel-generation system are linearized around an operating point as following:

$$p x = A x + B \mu + v d \quad (49)$$

Where

$$x = [X_1 \quad X_2]$$

and

$$X_1 = [\Delta i_{qs} \quad \Delta i_{ds} \quad \Delta i_{qr} \quad \Delta i_{dr} \quad \Delta \omega_m \quad \Delta v_{ds} \quad \Delta I_{DC} \quad \Delta i_q^r \quad \Delta i_d^r \quad \Delta i_{kd}^r]$$

$$X_2 = [\Delta i_{kd}^r \quad \Delta i_f^r \quad \Delta \omega_{sg} \quad \Delta \delta \quad \Delta V_c \quad \Delta V_f \quad \Delta \phi_r \quad \Delta \phi_f \quad \Delta x_1]$$

$$\mu = \begin{bmatrix} V_{Lref} & \omega_{sgref} \end{bmatrix}^t$$

$$d = [\Delta Z_L \quad v_w]$$

A = [a_{ij}] is a 19 x 19 matrix.

4. CONTROL STRATEGY

In this paper, the LQG controller has been employed to control the terminal voltage and frequency of an isolated hybrid wind-diesel generation unit. The LQG is a modern state space technique for designing optimal dynamic regulators. It has the following advantages:

- 1) It enables to trade off regulation performance and control effort.
- 2) It takes into account the process disturbance and measurement noise.

The LQG controller consists of an optimal state feedback gain “ k ” and a Kalman state estimator. The optimal feedback gain is calculated such that the feedback control law

$$u = -kx$$

minimizes the performance index :

$$H = \int_0^{\infty} (x^T Q x + u^T R u) dt$$

where Q and R are positive definite or semi definite Hermittian or real symmetric matrices. The optimal state feedback u = -kx is not implemental without full state measurement. In our case, the load current only is chosen to be the output measured signal. The Kalman filter estimator is used to drive the state estimation:

$$\hat{x} = [\hat{x}_1 \quad \hat{x}_2]$$

and

$$\hat{x}_1 = [\Delta \hat{i}_{qs} \quad \Delta \hat{i}_{ds} \quad \Delta \hat{i}_{qr} \quad \Delta \hat{i}_{dr} \quad \Delta \hat{\omega}_m \quad \Delta \hat{v}_{ds} \quad \Delta \hat{I}_{DC} \quad \Delta \hat{i}'_q \quad \Delta \hat{i}'_d \quad \Delta \hat{i}'_{kq}]$$

$$\hat{x}_2 = [\Delta \hat{i}'_{kd} \quad \Delta \hat{i}'_f \quad \Delta \hat{\omega}_{sg} \quad \Delta \hat{\delta} \quad \Delta \hat{V}_c \quad \Delta \hat{V}'_f \quad \Delta \hat{\phi}_r \quad \Delta \hat{\phi}_f \quad \Delta \hat{x}_1]$$

such that

$$u = -k\hat{x}$$

remains optimal for the output feedback problem. The state estimation is generated from [16]:

$$P = (A - Bk - LC)\hat{x} + Ly$$

Where L is the Kalman gain which is determined by knowing the system noise and choosing Q_n and R_n. However, the accuracy of the filter’s performance depends heavily upon the accuracy of this covariance. On the other hand the matrices A and B containing the hybrid wind diesel generation system parameters are not required to be very accurate due to the inherent feedback nature of the system. The Kalman filter performs best for linear systems. Therefore, the nonlinear model of the complete system has been linearized around an operating point. The optimal state feedback gains and the Kalman state space model have been calculated offline which results in great saving in computational burden. On this basis, the implementation of the proposed controller becomes easier and the hardware will be reduced to minimum.

5. SYSTEM CONFIGURATION

The block diagram of the isolated hybrid wind-diesel generation system with the proposed LQG controller is shown in Fig. 5. All the commanded values are superscripted with asterisk in the diagram. The LQG controller contains the Kalman state estimator in addition to optimal state feedback gains. The Kalman estimator uses both the measured d-q stator current components of induction generator and synchronous generator in order to estimate all the states including the d-q rotor current components of synchronous generator, generator speed of induction and synchronous machines, d-axis generated voltage at induction generator, DC link current, damper and field currents of synchronous generator, fuel flow rate of diesel engine. These states are multiplied by the corresponding optimal gains and summed to produce the control signals necessary to regulate the field voltage and the shaft rotational speed of the synchronous generator.

The entire system has been simulated on the digital computer using the Matlab/Simulink software package. The specifications of the system used in the simulation procedure are listed in appendix [12].

The noise and measurement covariance are set as :

$$Q_n = \text{diag} (10 , 10) \quad , \quad R_n = \text{diag} (1 , 1)$$

Also, the values of Q and R matrices which are necessary to calculate the optimal feedback gains are set as :

$$Q = \text{diag} (200 \ 10 \ 10 \ 10 \ 100 \ 10 \ 10 \ 10 \ 10 \ 100 \ 10 \ 10 \ 10 \ 10 \ 10 \ 10 \ 10 \ 1000) ,$$

$$R = \text{diag} (2.05 \ 2.05) .$$

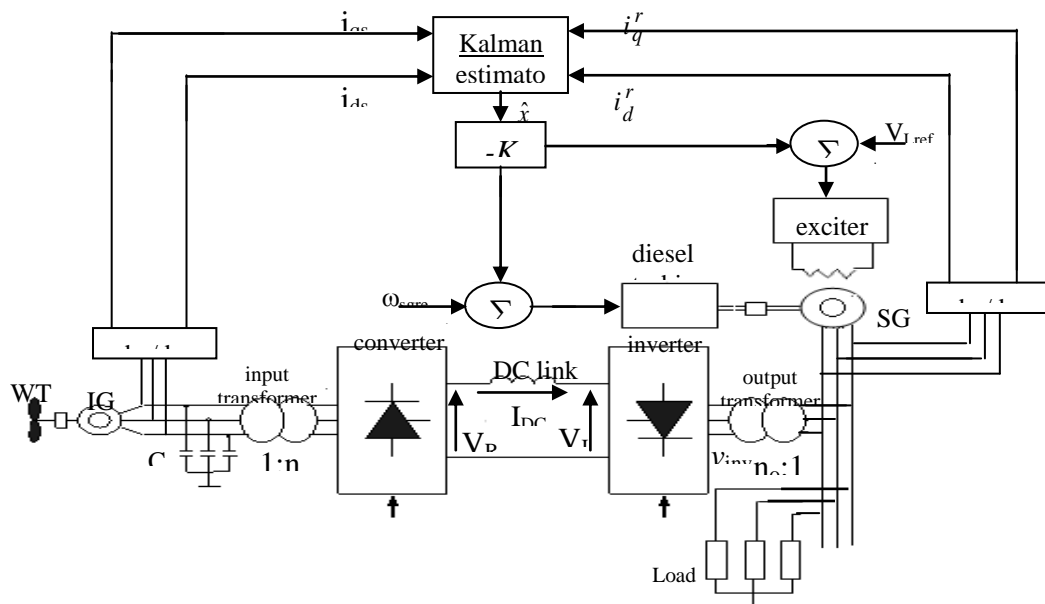


Fig. 5: Block diagram of the hybrid wind-diesel generation power system with the proposed LQG controller

6. SIMULATION RESULTS

Digital simulations have been carried out to validate the effectiveness of the proposed system under wind speed and load variations. The performance of the proposed scheme has been tested with a step changes in both wind speed and load impedance.

The simulation results depicting the variations in various variables with a step change in local load impedance is shown in Fig. 6. It is seen that as the local load impedance increases (the local current decrease), with wind velocity remaining constant, so the rotor speed of the synchronous generator tries to increase. The control action comes in operation and decreases the power output of the synchronous generator to meet the decreased power demand of the load. This is achieved by decreasing the diesel fuel rate ϕ_f which in turn decreases the torque (mechanical power) to the synchronous generator. Also, the field current is decreased to regulate the local bus voltage and the opposite will happen when the local impedance decreases.

The effect of variations in wind velocity on the various system variables are shown in Fig. 7. It seen that with increase in wind velocity (this means that the power contributed by the inverter increases) and hence the load voltage and current increase. So the same as the case of load impedance reduction, the controller comes in operation and reduces the diesel fuel rate ϕ_f which in turn decreases the torque (mechanical power) to the synchronous generator. Also the field current of the synchronous generator decreases. That leads to adjusting the load voltage and frequency and vice versa if the wind speed decreases. It is also seen that the damper winding current only comes into play during the initial transients, and reduces to zero subsequently. Simulation results indicate that a hybrid wind-diesel scheme can be adequately controlled and the local bus voltage and frequency can be regulated by the use of AVR and a diesel engine with robust LQG control.

7. CONCLUSIONS

This paper investigates the robust control of an isolated wind-diesel generation system based on the LQG approach. The controlled system consists of a diesel engine that drives a synchronous generator connected to an isolated load and the synchronous generator is equipped with an automatic voltage regulator (AVR) and a static exciter and also wind turbine driven SEIG, which interfaced to the load bus through DC-link. A complete model, control design and simulations of this scheme have been developed showing the ability of the controller to compensate both the wind power oscillations and load disturbances. The local load bus voltage and frequency are governed by the synchronous machine. The load bus voltage is regulated via controlling the field current of the synchronous generator. Also, the load bus frequency is adjusted by controlling the rotor speed of the synchronous generator which is adjusted by controlling the diesel fuel flow rate ϕ_f which in turn affects the torque (mechanical power) input to the synchronous generator and hence its rotation speed. The standard Kalman filter technique has been used to estimate the full states of the system by measuring only the currents of both induction and synchronous generators. The proposed controller has the advantages of robustness, easy implementation and adequate performance in face of uncertainties.

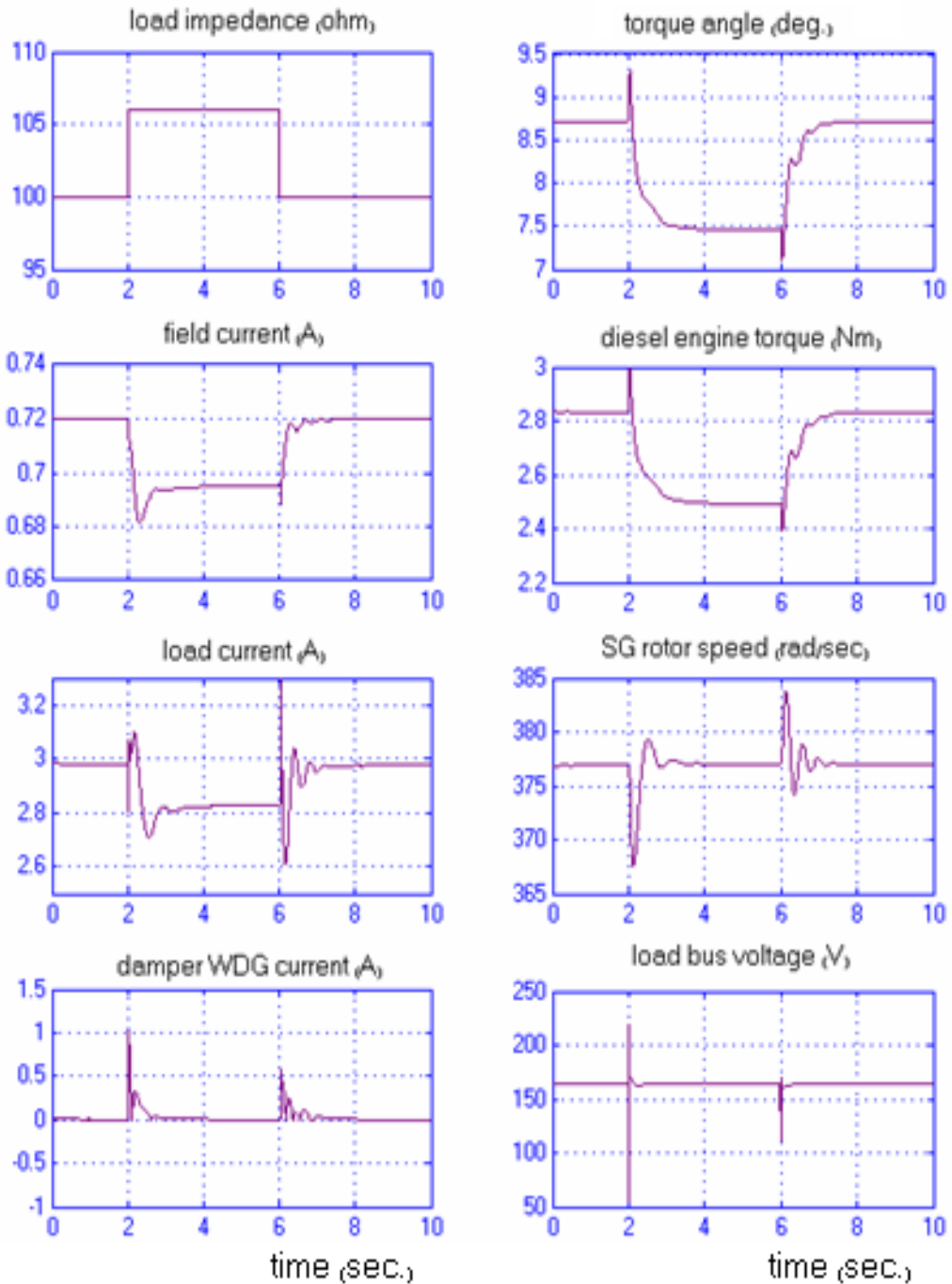


Fig. 6: Dynamic response of the proposed system with a step change in load impedance.

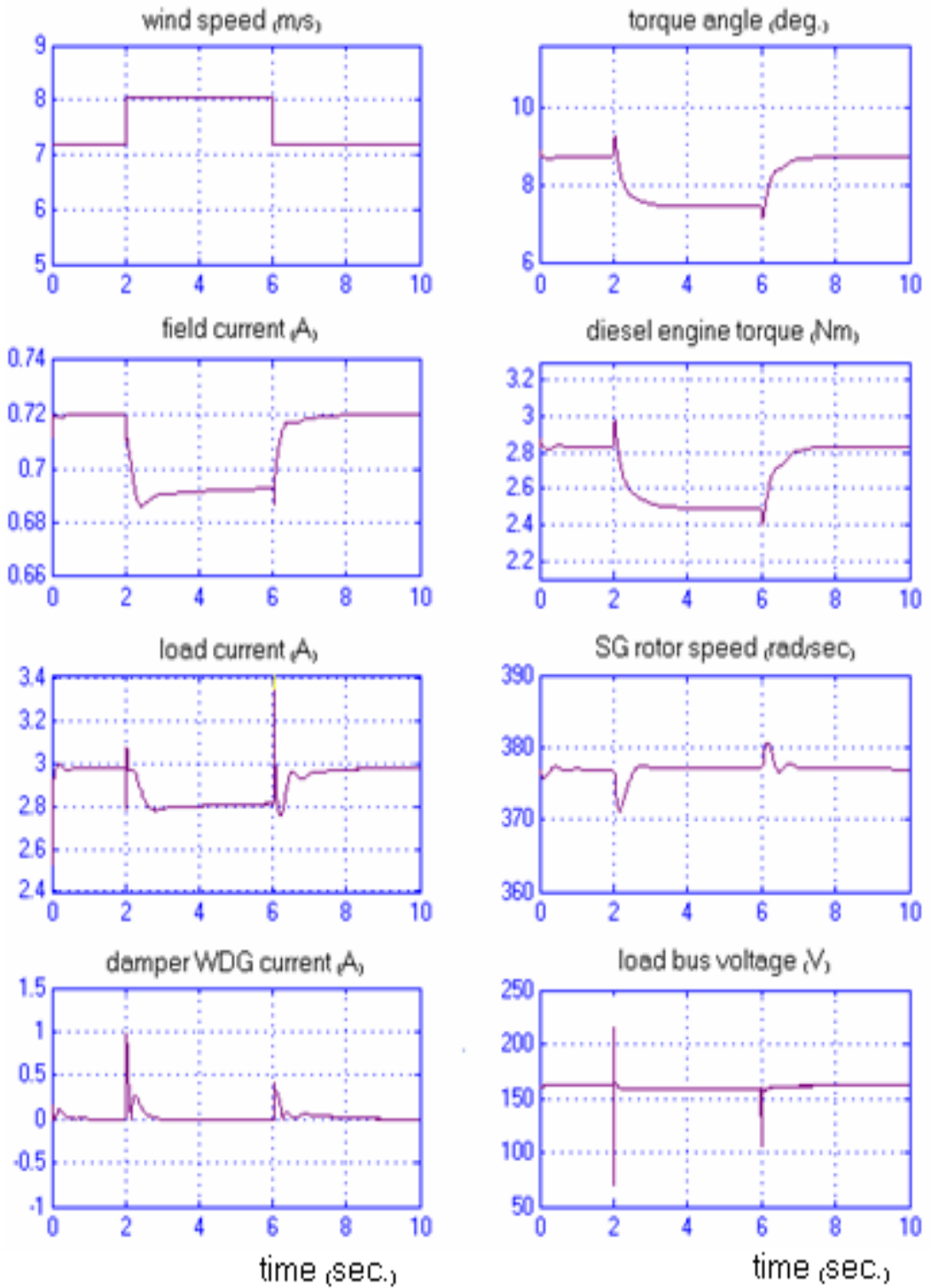


Fig. 7: Dynamic response of the proposed system with a step change in wind speed.

Digital simulations have been carried out in order to evaluate the effectiveness of the proposed scheme. The wind-diesel energy system with the proposed controller has been tested through step changes in wind speed and load impedance. The results prove that the proposed controller is successful in regulating the terminal voltage and frequency of a stand alone wind-diesel energy conversion system under wind and /or load excursion.

8. REFERENCES

- [1] J. T. Bialasiewicz, E. Muljad and S. Drouilhet , "Modular Simulation of a Hybrid Power System with Diesel and Wind Turbine Generation". Presented at Windpower '98 Bakersfield, CA, National Renewable Energy Laboratory, April 27-May 1, 1998.
- [2] W.E.Leithead, SA.De La Salle and D. Reardon, "Classical Control of Active Pitch Regulation of Constant Speed Horizontal Axis Wind Turbines", International Journal of Control, Vol.55, No.4, pp.845-876, 1992
- [3] Hussein Ibrahim, Adrian Ilinca, Rafic Younès, Jean Perron and Tammam Basbous " Study of a Hybrid Wind-Diesel System with Compressed Air Energy Storage", IEEE, Electrical Power Conference, EPC2007, Montreal, Canada, pp. 25-26, October 2007.
- [4] Bansal, R.C., "Automatic Reactive-Power Control of Isolated Wind–Diesel Hybrid Power Systems". IEEE Trans. On Industrial Electronics, V 53. Issue 4, pp. 1116-1126, June 2006.
- [5] G.W.Scott, V.F.Wilreker and R.K.Shaltens, "Wind Turbine Generator Interaction With Diesel Generators on an Isolated Power System" IEEE Trans. on Power Apparatus and Systems, V. PAS-103, No.5, pp.933-937, May 1984.
- [6] Bansal, R.C, Bhatti, T.S and Kothari, D.P. " Automatic reactive power control of wind-diesel-micro-hydro autonomous hybrid power systems using ANN tuned static VAr compensator". Large Engineering Systems Conference on Power Engineering, V 7. pp. 182-188. May 2003.
- [7] Panickar, PS, Rahman, MS and Islam, S., " A Neuro-fuzzy Model for the Control Operation of a Wind-diesel-battery Hybrid Power System". Journal of Electrical & Electronics Engineering, V 22, Issue 1, pp. 9-16, Australia, 2003.
- [8] JURADO Francisco and SAENZ José R., "Neuro-fuzzy control for autonomous wind–diesel systems using biomass". Journal of Renewable Energy, V 27, Issue , 1,pp. 39-56, September 2002.
- [9] Chedid, R.B.; Karaki, S.H.; El-Chamali, C. "Adaptive fuzzy control for wind-diesel weak power systems".IEEE Trans. on Energy Conversion, V 15, Issue 1, pp. 71-78, Mar 2000.
- [10] Pena, R., Cardenas, R., Proboste, J., Clare, J. and Asher, G. "A hybrid topology for a variable speed wind-diesel generation system using wound rotor induction machines". Industrial Electronics Society, 2005. IECON 2005. 31st Annual Conference of IEEE, 6-10 Nov. 2005.
- [11] A. Abdin and X. Wilson, " Control design and dynamic performance analysis of a wind turbine-induction generator unit", IEEE Trans. On Energy Conversion, Vol. 15, No. 1, March, 2000, pp 91-96.

- [12] R. M. Hilloowala, "Control and interface of renewable energy systems", Ph.D. Thesis, The University of New Brunswick, Canada, 1992.

9. Appendix

Synchronous Machine parameters:

Rating: 2 KW, 208 V (line), 9 A, 4 pole, Unity power factor.

Constants: $R_s=0.88 \Omega$, $R_f=67.0 \Omega$, $L_{md}=58 \text{ mH}$, $L_{mq}=24.9 \text{ mH}$, $L_{lsd}=L_{lsq}=2.92 \text{ mH}$, $L_{lfd}=2.92 \text{ mH}$

$N_{se} : N_{fd} = 0.047 : 1$

$N_{se} : N_{kd} = 2.95 : 1$

$N_{se} : N_{kq} = 2.95 : 1$

Wind turbine :

Rating : 1 kw , 450 rpm (low speed side) at $V_w = 12 \text{ m/s}$.

Size : Height = 4 m , Equator radius = 1 m , Swept area = 4 m^2 , $\rho = 1.25 \text{ kg/m}^3$.

Induction machine :

Rating : 3-phase , 2 kw , 120 V , 10 A , 4-pole , 1740 rpm .

Parameters : $R_s = 0.62 \Omega$, $R_r = 0.566 \Omega$, $L_s = L_r = 0.058174 \text{ H}$, $L_m = 0.054 \text{ H}$,

$J = 0.0622 \text{ kg.m}^2$,

$f = 0.00366 \text{ N.m./rad/s}$.

DC Link : $R_{DC} = 1.7 \Omega$, $L_{DC} = 0.15 \text{ H}$.

Self Excitation Capacitor:

Rating : $176 \mu\text{f}$ / phase , 350 V , 8 A .

التحكم المتين في منظومة قوي كهربية للرياح والغاز المعزولة باستخدام منظم جاوسان الخطي

تزايدت الاهتمامات في السنوات الاخيرة الي استخدام الطاقة الجديدة والمتجددة في توليد الطاقة الكهربية وخاصة من طاقة الرياح خاصة في المناطق النائية والتي يصعب ربطها بالشبكة الكهربية. ونظرا لعدم ضمان استمرار الرياح او عدم ضمان استمرار الطاقة الكهربية الكافية المولدة من طاقة الرياح لذلك نلجأ الي انظمة التوليد المختلطة. يتعرض هذا البحث الي استخدام التحكم التريبعي الخطى لجاوس (Linear Quadratic Gaussian Control) وذلك في تغذية حمل معزول (غير مربوط بالشبكة الكهربية) من نظام توليد كهربي مختلط مكون من وحدتي توليد للكهرباء. الوحدة الأولى مكونة من مولد حثي مدار بتوربينة رياح ومتصل بالحمل من خلال (DC-Link) غير محكوم للحصول علي أقصى قدرة يمكن توليدها من طاقة الرياح. والوحد الثانية مكونة من مولد متزامن مدار بمحرك ديزل.

تم تمثيل النظام بنموذج رياضي غير خطي تم توصيفه وتحويله إلي نموذج رياضي خطي حول نقطة تشغيل محددة مسبقا. تم تثبيت الجهد والتردد علي أطراف الحمل وذلك بالتحكم في جهد وتردد خرج المولد المتزامن بالتحكم في جهد تغذية ملفات المجال والتحكم في السرعة الدورانية للمولد المتزامن علي التوالي وذلك باستخدام التحكم التريبعي الخطى لجاوس . في هذه الطريقة يتكون هيكل الحاكم من جزئين اساسيين هما : مرشح كالمان (Kalman Filter) ، والكسب المثالي لمتغيرات النظام . وقد تم استخدام مرشح كالمان في تقدير جميع متغيرات النظام المحكوم وضربها في الكسب المثالي لإيجاد الإشارة الحاكمة. هذه الإشارة يتم إضافتها إلى النظام المحكوم باستخدام التغذية العكسية. وقد تم استخدام إشارة تيار العضو الثابت لكل من المولد الحثي والمولد المتزامن كدخل لمرشح كالمان لأنه من السهل قياسها واستخدام المرشح في تقدير باقي متغيرات النظام والتي يصعب قياسها.

تم اختبار اداء الحاكم وذلك بعمل اضطراب للنظام بتغيير كل من سرعة الرياح ومعاوقة الحمل، وبحساسيته وقوته ضد تغير قيم بيانات النظام.